

<https://doi.org/10.21608/sjsoci.2024.267140.1178>

Histological and Histopathological Changes Induced by Melanin Extracted from *Sepia pharaonis*' Ink on Some Organs of Pigmented and Albino Mice and the Role of Glutathione

Alaa Y. Moustafa*, Basma Abd El-Naser, Aziz Awaad

Department of Zoology, Faculty of Science, Sohag University, Sohag 82524, Egypt

*Email: alaa.moustafa@science.sohag.edu.eg

Received: 12th February 2024, Revised: 8th May 2024, Accepted: 22nd May 2024

Published online: 21st June 2024

Abstract: The current investigation provided the first more detailed study into the comparative histopathological and hematology changes induced by melanin extracted (ME) from *Sepia pharaonis*' ink in both albino and pigmented mice. Additionally, the role of glutathione (GSH) as a melanin-control drug has been investigated when administered simultaneously with ME. *S. pharaonis*' ME had harmful effects on the mammalian digestive system at the current dose (25 mg/kg). In hepatocytes, it causes inflammation with lymphocyte aggregation from damaged cells and vacuolation deformation at the stomach, colon, liver, and spleen. However, the skin showed an increase in hair follicle number and some inflammations. The administration of ME showed an increase in blood platelets and elevation of lymphocytes. The co-administration of GSH simultaneously with ME reduced some of these abnormalities. ME showed a greater influence on the treated spleen and skin compared with those treated with both ME and GSH. Additionally, the effect of GSH treatment concurrently with ME controlled these alterations and decreased inflammation, as well as vacuolation. The present study highlights some in vivo negative parameters produced by ME extracted from *S. pharaonis*, and this may be useful for people who eating foods containing ink. Additionally, more investigations are needed to illustrate the importance of ME when it is used in skincare cosmetics.

Keywords: Cuttlefish, melanin, histopathology, biochemical, spleen, skin, hair follicle, antioxidant.

1. Introduction

Cephalopods are soft-bodied marine molluscs; they constitute a famous source of food components. The ink of cephalopods is used as food. The most prevalent application is as a food flavoring, which is used worldwide. Because of its excellent flavor, cuttlefish ink is used in the majority of commercial squid inks [1] as well as processed inks are used in food coloring [2]. Because of its antibacterial properties, cuttlefish ink is also used cuttlefish meat preservative, to extend its shelf life [3, 4], it also used traditionally in Mediterranean diet [5] or south-Asian culinary preparations [6] and in special occasions for some ethnic groups [7].

Cephalopod ink is composed of two main ingredients, black ink secretes from the ink sac and mucus secretes from the funnel organ [4]. The ink is chemically composed of melanin, proteins, peptides, glycosaminoglycan, and certain enzymes such as tyrosinase, dopamine and L-DOPA. In addition, it contains lipids, heavy metals and lower levels of amino acids such as aspartic acid, taurine acid, glutamic acid, lysine and alanine [8].

Cephalopods melanin extract (ME) showed many biological activities such as antioxidant [9, 10], anti-microbial [10-14], and anti-inflammatory [15], and chemo-

prophylactic activities [16]. Moreover, ME from cephalopods inhabited the gastric juice secretions in rats [17-19]. The binding characteristics of neuromelanin in Parkinson's disease model was studied using *Sepia's* ME [20].

Glutathione (GSH) is considered as an antioxidant [21]; it has a vital role to reduce the toxicities of drugs and xenobiotics [22]. It plays a role in detoxification of hydrogen peroxide as a hydrogen donor. In addition, GSH plays a role in improving liver abnormalities [23, 24]. As a result, GSH can be used as a food or health supplement, as well as a pharmaceutical agent. It is even used to treat autistic children [25].

The purpose of the current investigation is to give a comparative study on the histopathological abnormalities induced by ME extracted from *S. pharaonis*' ink and the ameliorative role of GSH after oral administration into albino and pigmented mice. These histopathological tests were performed on five mammalian tissues including the liver; as a detoxifier organ that breaks down poisons, narcotics, other substances and xenobiotics [26]. Additionally, the spleen which is the biggest lymphatic organ followed by the colon and stomach which are responsible for absorption and mucosal immunity. Finally, it

applied to the skin which is used to assess the effect of melanin on hair follicles and the skin in general.

2. Materials and methods

2.1. Materials

Hematoxylin and eosin stains were bought from Sigma-Aldrich (Ontario, Canada). GSH source was from Alpha Hepadox capsules, each capsule contains 200 mg of GSH per capsule (Zoser Pharma, Egyptian Company). The rodent chow used for daily feeding of rodents was obtained from Feed Mix Egypt Co, El Obour town, El- Qalyubia Governorate, Egypt.

2.2. Cuttlefish collection and melanin extraction

The fresh cuttlefish, *S. pharaonis* were collected from Hurghada coastal waters by a fisherman, Red Sea Governorate, Egypt. They were transported to the Department of Zoology, Faculty of Science, Sohag University in an icebox. Ink sacs of cuttlefish were dissected out. Inks were removed from the ink sacs, and they were diluted by cold distilled water (4°C), it was then centrifuged (three times) at 18,000 RPM for 30 minutes at 4°C in a refrigerated centrifuge. The obtained supernatant was termed as "melanin-free ink". The remaining precipitate melanin (ME) was immediately frozen and kept at -20°C [27] sequentially. Lyophilization was carried out in a freeze dryer, then, ME was obtained and later it was characterized using infrared (IR) spectroscopy. The cuttlefish *S. pharaonis* were identified according to Riad [28].

2.3. Experimental design

Male adult albino mice (*Mus musculus*) were used as an experimental model for this study. The mice were purchased from Animal House, Department of Zoology, Faculty of Science, Sohag University, and Sohag Governorate, Egypt. Male-pigmented mice (C57BL/6) weighted about 25 ± 2 g, were purchased from Animal House, Cairo University, Cairo Governorate, Egypt. Animals were housed in a ventilated animal house at ($25 \pm 2^\circ\text{C}$; 12 h light/dark regime). Mice were supplied with clean water and food regularly and left to acclimatize for 6 days prior to the experiment. All animal experiments were performed under the guidelines and ethics approved by the Animal Experiment Committee at the Department of Zoology, Faculty of Science, Sohag University (Protocol No: CSRE-3-23).

A total number of 15 adult albino mice and 15 adult pigmented mice were used for this experiment. Both Albino mice and pigmented mice were divided randomly into 3 groups as follows: The 1st group (negative control) received a standard mice chow diet and water. The 2nd group (ME group) was orally administrated with ME (25 mg/kg) for 3 weeks using animal feeding gavage [24]. The 3rd group (ME + GSH group) was orally administrated with GSH (100 mg/kg) for 5 weeks and simultaneously ME (25 mg/kg) was injected for 3 weeks starting from the 2nd week of GSH injection. At the targeted time point, animals of all groups were anesthetized using an overdose of diethyl ether and

carefully dissected. Small parts of the liver, spleen, skin, stomach, and colon were obtained from each mouse for routine histology.

2.4. Histological investigations

For hematoxylin and eosin (H&E), each organ was fixed in Carnoy's fixative. Tissues were dehydrated in an ascending series of ethyl alcohol. They were cleared in methyl benzoate and toluene and then embedded in paraffin for six hours. Sections of 5-7 μm were obtained using rotary microtome. Sections were mounted on clean glass slides deparaffinized with xylene and dehydrated in a descending series of alcohol. Sections were stained with H&E, DPX-mounted, covered with glass slide covers, and viewed under a light microscope [29].

2.5. Biochemical analysis

The blood was collected from each animal using EDTA-containing blood vials and then analyzed using hematology analyzer (HA-Vet clinging system BVBA, Belgium) to measure the levels of the following parameters: Hemoglobin (HGB), red blood corpuscles (RBCs) numbers, mean corpuscular hemoglobin (MCH), mean corpuscular volume (MCV), mean corpuscular hemoglobin concentration (MCHC), blood platelet numbers, and lymphocytes numbers.

3. Results

3.1. Histopathological examinations of the liver

3.1.1. Liver of albino mice

The control liver of albino mice showed normal histological architectures with normal hepatic parenchyma. Hepatocytes showed normal nuclei and cytoplasm. Hepatic blood vessels showed normal bio-distribution and appearance (Fig. 1 A, B, and C). After 3 weeks of ME administration, the liver showed severe degeneration and vacuolation in the hepatocyte's cytoplasm, diameters enlargement, and congestion in most of the hepatic portal vein as well as mild dilation of the blood vessels (Fig. 1 D, E, and F). Cytoplasmic degeneration and vacuolation slightly decreased after co-administration of both GSH and ME as compared with only ME administration (Fig. 1 G, H, and I). In general, the histological structure of the liver slightly improved after the co-administration of GSH with ME.

3.1.2. Liver of pigmented mice

Similar to albino mice, a normal histological architecture with intact hepatic strands and hepatocytes was observed in the control liver of pigmented mice (Fig. 2 A, B, and C). After 3 weeks of ME administration, some lymphocyte aggregations within the hepatic parenchyma as well as cytoplasmic vacuolation were observed. Additionally, degeneration and vacuolation in the hepatocyte's cytoplasm, enlargement, and congestion of the hepatic portal vein was observed after administration of ME (Fig. 2 D, E, and F). Compared with the ME-treated group, the number of lymphocyte aggregations decreased around both the hepatic

portal vein and central veins after 5 weeks of GSH simultaneously administered with ME (Fig. 2 G, H, and I).

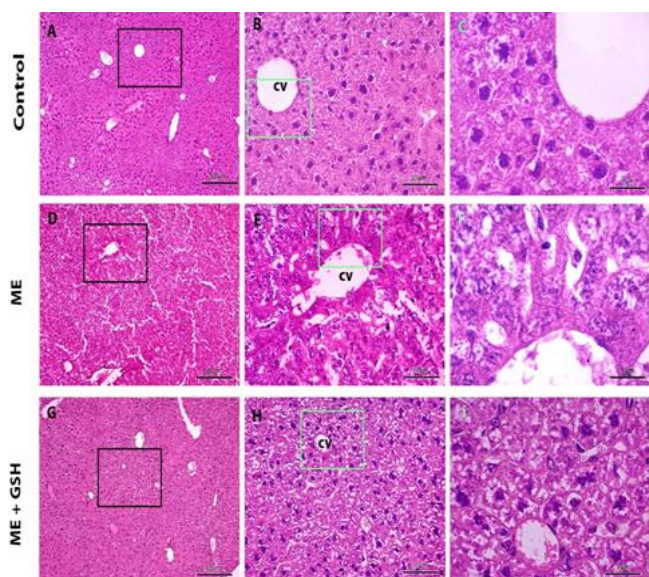


Figure 1: Photomicrographs from sections of albino mice liver stained with H&E. A, B, and C: Control liver with normal structure. D, E, and F: after 3 weeks of ME injection showing blood vessel dilation and cellular vacuolation. G, H, and I: after 5 weeks of GSH and ME administration showing a decrease of lymphocytic infiltration (bold arrows), vacuolar degeneration (arrowheads), dilation and congestion of the central vein (arrow) and basophilic affinity of the cytoplasm. Abbreviations: CV = central vein. Scale bar: A, D, and G = 50 μ m; B, E, and H = 10 μ m and C, F, and I = 5 μ m.

3.2. Histopathological examinations of the spleen

3.2.1. Spleen of albino mice

The control spleen of albino mice showed normal histological architectures. Mainly, the spleen is composed of two parts white pulp and red pulp. The white pulp is a lymphatic follicle, containing mainly lymphocytes. The red pulp surrounds the white pulp and contains erythrocytes and immune cells (Fig. 3 A, B, and C). The ME treatment showed different histopathological changes in the spleen after 3 weeks of administration. Additionally, several aggregations of lymphocytes infiltrations were seen scattered in the spleen red pulp, as well as higher number of megakaryocytes, and distortion in the shape of spleen follicles compared to those in the control group (Fig. 3 D, E, and F). Administration of GSH simultaneously with ME showed slightly reduced abnormalities induced by ME extract treatment only (Fig. 3 G, H, and I). As a result, our study showed that GSH can regulate the irregularities caused by ME treatment.

3.2.2. Spleen of pigmented mice

The spleen of control pigmented mice showed normal histological structures with normal splenic cells and intact spleen follicles with normal white and red pulps with intact hepatic strands and hepatocytes (Fig. 4 A, B, and C). There

are no obvious differences between the histological structure of the control spleen in albino and pigmented mice.

The oral administration ME showed several histopathological abnormalities after 3 weeks (Fig. 4 D, E, and F). These abnormalities include lymphocytes aggregations scattered in the spleen red pulp, while, after 5 weeks of simultaneous GSH administration, ME spleen showed a lower number of lymphocyte infiltration (Fig. 4 G, H, and I).

After 3 weeks of ME administration (Fig. 4 D, E, and F), the spleen showed a higher number of megakaryocytes and distortion in the follicle shape compared to those in the control group. As a result, after 5 weeks of administration of (GSH and ME), this group exhibited better histological structures than the second group of ME administration.

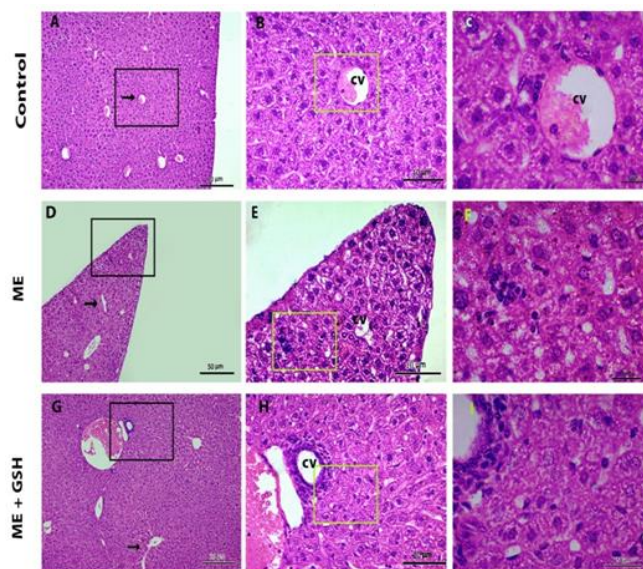


Figure 2: Photomicrographs from sections of pigmented mice liver stained with H&E. A, B, and C: Normal structure of control liver. D, E, and F: after 3 weeks of ME administration showing lymphocytic infiltration, blood vessel dilation and vacuolation degeneration in the hepatocytes G, H, and I: after 5 weeks of GSH and ME administration showing a decrease of lymphocytic infiltration (bold arrows), vacuolar degeneration (arrowheads), dilation and congestion of the central vein (arrow) and basophilic affinity of the cytoplasm. Abbreviations: CV = central vein. Scale bar: A, D, and G = 50 μ m; B, E, and H = 10 μ m and C, F, and I = 5 μ m.

3.3. Histopathological examinations of the skin

3.3.1. Skin of albino mice

The control skin of albino mice showed normal histological structures with normal melanocyte bio-distribution (Fig. 5 A, B, C, and D). After 3 weeks of ME administration, the skin showed inflammation with lymphocyte aggregation, some damaged cells, and vacuolation (Fig. 5 E, F, G, and H). After 5 weeks of GSH and ME administration, some cells showed slight vacuolation and lymphocyte aggregation and tissue showed

less inflammatory response (Fig. 5 I, J, K, and L). Additionally, the number of hair follicles increased after 3 weeks of administration of ME compared to normal skin or after 5 weeks of GSH administration and ME.

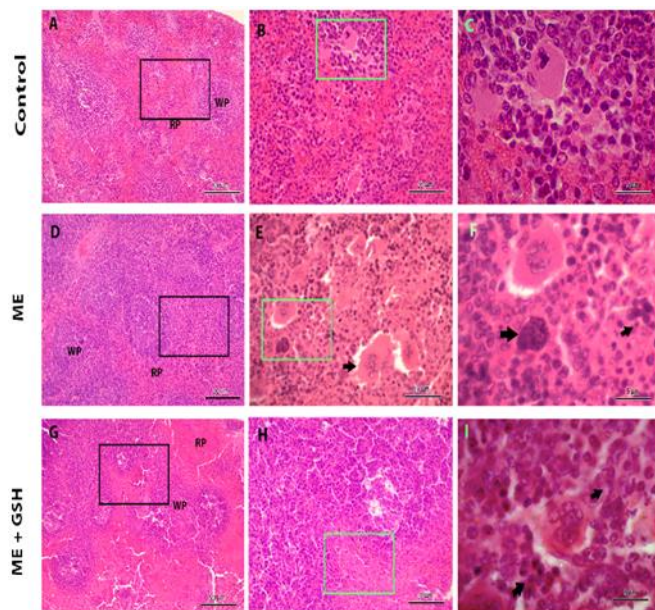


Figure 3: Photomicrographs from sections of albino mice spleen. A, B, and C: normal spleen structure. D, E, and F: after 3 weeks of ME administration showing an elevation of megakaryocytes numbers, mild infiltration of the lymphoid cells (arrows) and mild follicle shape distortion. G, H, and I: after 5 weeks of GSH and ME administration showing a decrease of lymphocytic aggregations (arrows) within the red pulp, and follicle shape distortion. Abbreviations: RP: red pulp; WP: white pulp. Scale bar: A, D, and G = 50 μ m; B, E, and H = 10 μ m and C, F, and I = 5 μ m.

3.3.2. Skin of pigmented mice

The pigmented mice's skin showed normal histological architecture with normal melanocyte bio-distribution (Fig. 6 A, B, C, and D). The tissue structure of the normal skins of albino and pigmented mice are semi-identical.

Following the administration of ME for three weeks, inflammation was seen along with lymphocyte aggregation from harmed cells and vacuolation (Fig. 6 E, F, G, and H). Sections exhibit a reduced inflammatory response after 5 weeks of GSH and ME with minor vacuolation and lymphocyte aggregation (Fig. 6 I, J, K, and L). The third group (GSH + ME) demonstrated improvement in the tissue inflammation and abnormalities compared to those of the second group (ME only).

3.3.3. Skin of pigmented mice

The pigmented mice's skin showed normal histological architecture with normal melanocyte bio-distribution (Fig. 6 A, B, C, and D). The tissue structure of the normal skins of albino and pigmented mice are semi-identical.

Following the administration of ME for three weeks, inflammation was seen along with lymphocyte aggregation

from harmed cells and vacuolation (Fig. 6 E, F, G, and H). Sections exhibit a reduced inflammatory response after 5 weeks of GSH and ME with minor vacuolation and lymphocyte aggregation (Fig. 6 I, J, K, and L). The third group (GSH + ME) demonstrated improvement in the tissue inflammation and abnormalities compared to those of the second group (ME only).

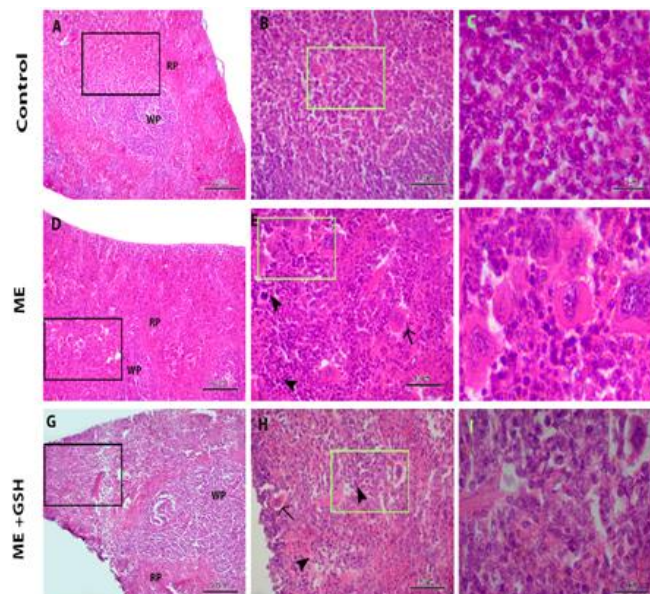


Figure 4: Photomicrographs from sections of pigmented mice spleen stained with H&E. A, B, and C: showing control spleen with normal architecture. D, E, and F: after 3 weeks of ME administration showing an increase of megakaryocytes (arrows), mild aggregations of the lymphoid cells (bold arrows) and mild follicle shape distortion. G, H, and I: after 5 weeks of GSH + ME administration showing a decrease of lymphocytic aggregations within the red pulp (bold arrows), and follicle shape distortion. Abbreviations: RP: red pulp; WP: white pulp. Scale bar: A, D, and G = 50 μ m; B, E, and H = 10 μ m and C, F, and I = 5 μ m.

Quantitative analysis of hair follicles

Figure 7 showed the changes in the number of hair follicles following administration of ME (Group 2) and GSH + ME administration (Group 3), compared to the control. After 3 weeks, the ME showed a significant increase in the number of hair follicles in albino mice and in pigmented mice. After 5 weeks of GSH + ME treatment, the number of hair follicles improved and became comparable to the control group.

3.4. Histopathological examinations of the stomach

3.4.1. Stomach of albino mice

The histological structures stomach of the control albino mice showed normal architectures. The gastric glands appeared as equal deep cavities perpendicular to the stomach wall. Each pit has several tiny straight tubular ducts that emerge into it (Fig. 8 A, B, and C).

Sections of albino mice stomach after 3 weeks of ME administration (Fig. 8 D, E, and F) showed inflammations

and lymphocyte aggregations from damaged cells in the lamina propria area. Vacuolation, distortion in the mucosal epithelium and detachment of lamina propria were observed. After 5 weeks of GSH and ME administration, vacuolations and lymphocyte aggregations were decreased (Fig. 8 G, H, and I). Consequently, the third group (GSH and ME) demonstrated an obvious improvement in histological structure after 5 weeks of administration compared to the second group.

3.4.2. Stomach of pigmented mice

The stomach of control pigmented mice showed normal architectures (Fig. 9 A, B, C and D). There is no variation in the histological structure of albino and pigmented mice's normal stomach. After 3 weeks of ME administration (Fig. 9, E, F, G and H), inflammation with lymphocyte aggregation from damaged cells, cytoplasmic vacuolation, distortion in the mucosal epithelium, and detachment of lamina propria were observed. (Fig. 9 I, J, K, and L) after 5 weeks of GSH and ME administration, vacuolation and lymphocyte aggregation decreased. Finally, after 5 weeks of administration, the third group (GSH and ME) had a somewhat normal histological structure.

3.5. Histopathological examinations of the colon

3.5.1. Colon of albino mice

The colon of control albino mice has normal columnar cells and many goblet cells. The muscular mucosa forms the core of each villus and fill the spaces between glands. Each villus contains a central lymph vessel and the lacteal (Fig. 10 A, B, C, and D). After 3 weeks of ME extract administration, cross sections of colon showed inflammation with lymphocyte aggregation from damaged cells and detachment from the epithelium (Fig. 10 E, F, G, and H). After 5 weeks of GSH and ME administration, a decrease in vacuolation and lymphocyte aggregations were observed (Fig. 10 I, J, K, and L), compared with the colon after 3 weeks of administration of ME.

3.5.2. Colon of pigmented mice

Likewise, sections of pigmented mice colon showed normal architecture like albino mice (Fig. 11 A, B, C, and D). After 3 weeks of ME administration, the treated colon showed inflammation with lymphocyte aggregation from damaged cells. (Fig. 11 E, F, G, and H). After 5 weeks of GSH and ME administration, a decrease in cellular vacuolation and lymphocyte aggregation compared with treated colon ME only for 3 weeks (Fig. 11 I, J, K, and L) was observed.

3.6. Biochemical analysis

Figures 12 and 13 showed the changes in hematological parameters following ME (Group 2) and GSH + ME (Group 3) treatments. When compared to the control, after three weeks, the ME revealed a decrease in HGB, RBCs count MCV, MCHC, and MVC, as well a significant increase in platelets and lymphocytes of both albino and pigmented mice. However, after 5 weeks of GSH and ME

administration, exhibited increments of HGB, RBCS count, MCV, MCHC, and MVC. A significant decrease is noted in platelets of both albino mice and pigmented mice compared to group one, while lymphocytes of albino mice were significantly decreased.

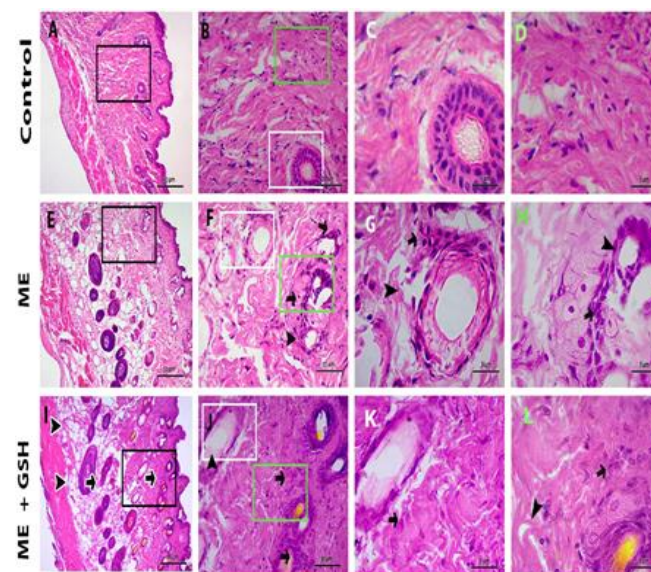


Figure 5: Photomicrographs from sections of albino mice skin stained with H&E. A, B, C, and D: showing control skin with normal architecture and melanocytes bio-distribution. E, F, G, and H: after 3 weeks of ME administration showing inflammation with lymphocytes aggregation (arrows) from damaged cells and vacuolation (arrows heads). I, J, K, and L: after 5 weeks of GSH+ME administration showing slight vacuolation and lymphocytes aggregation, sections show less inflammatory respond. C, G, and K: hair follicles sowing erosions. Scale bar: A, E, and I = 50 μ m; B, F, and J = 10 μ m and C, D, G, H, K, and L = 5 μ m.

4. Discussion

The current study provided the first new understanding of the comparative histopathological alterations induced by a single dose (25 mg/kg) of ME extracted from ink of *S. pharaonis* in both albino and pigmented mice. Additionally, the ameliorative role of GSH, as a medication that controls melanin, when administered alongside with ME is studied.

The main distinction between melanocytic and albino animals is that melanocytic denotes an abundance of pigmentation enzymes, whereas albino denotes a lack of pigmentation enzymes [30, 31].

The histological abnormalities in the liver parenchyma after oral injection of ME include lymphocyte aggregations, vacuolar degeneration and congestion and enlargement of the hepatic portal vein tissues. *S. pharaonis* ME caused negative impacts on mammalian hepatocytes at the current concentration (25 mg/kg) in both albino and pigmented mice. Similarly, 5, 6-dihydroxy indole (DAI) as one of ME compositions was shown to be cytotoxic for non-melanocytic cells and had no discernible impact on melanoma cells [32, 33].

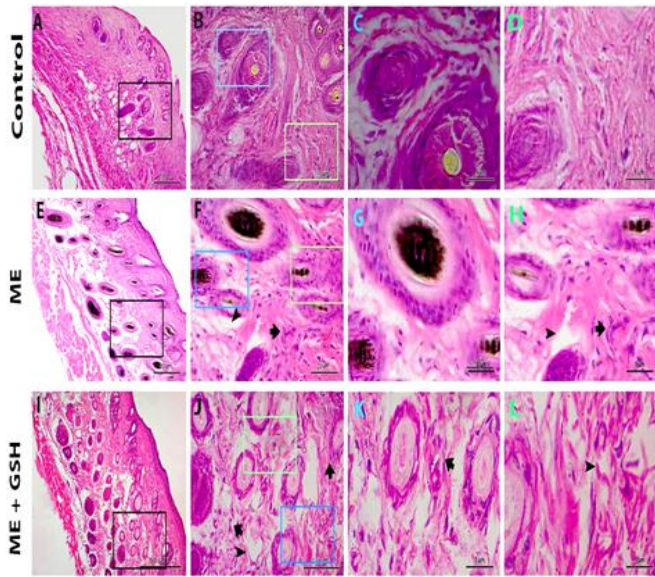


Figure 6: Photomicrographs from sections of pigmented mice skin stained with H&E. A, B, C, and D: showing control skin with normal architecture and melanocytes bio-distribution. E, F, G, and H: after 3 weeks of ME administration-showing inflammation with lymphocytes aggregation (arrows) from damaged cells and vacuolation (arrows heads). I, J, K, and L: after 5 weeks of GSH + ME administration showing slight vacuolation and lymphocytes aggregation, sections show less inflammatory respond. C, G, and K: comparison between hair follicles which showing erosion. Scale bar: A, E, and I = 50 μ m; B, F, and J = 10 μ m and C, D, G, H, K, and L = 5 μ m.

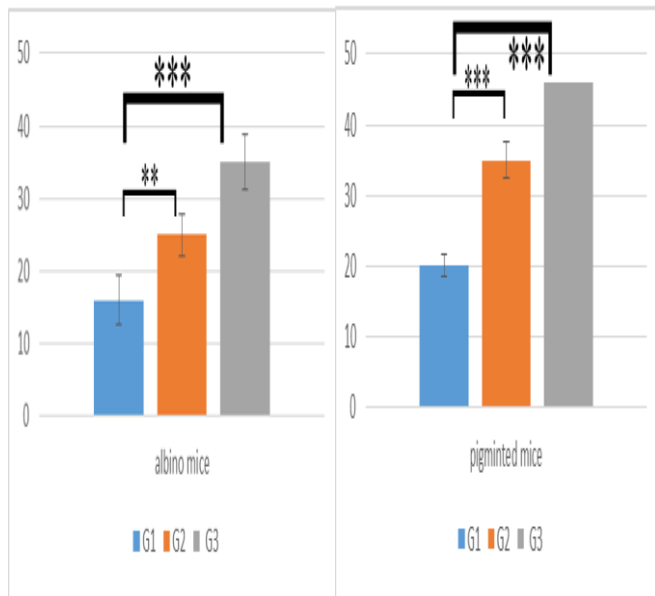


Figure 7: Semi-quantitative analysis of the modifications in albino and pigmented mice hair follicles: G1 control. G2: After 3 weeks of ME administration showing a substantial increase in the number of hair follicles ($p \leq 0.01$) in albino mice and ($p \leq 0.001$) in pigmented mice. G3: After 5 weeks of GSH + ME administration, the number of hair follicles was improved ($p \leq 0.001$) in albino mice and ($p \leq 0.001$) in pigmented mice.

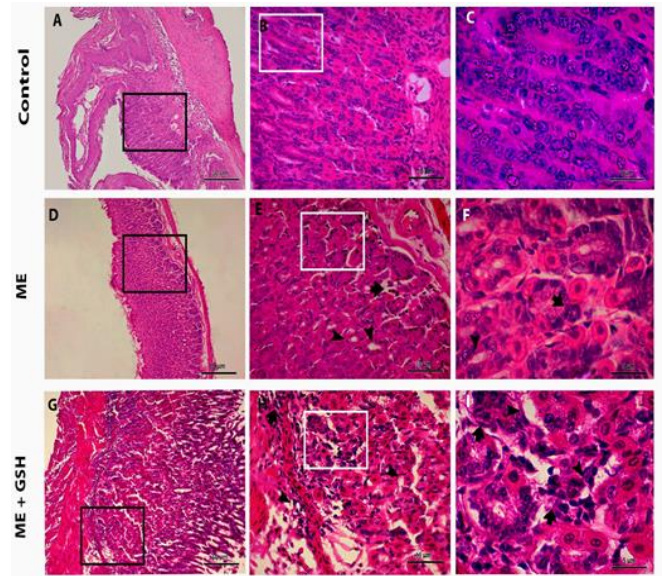


Figure 8: Photomicrographs from sections of albino mice stomach stained with H&E. A, B, and C: showing control stomach with normal architecture. D, E, and F: after 3 weeks of ME administration showing inflammation with lymphocytes aggregation (arrows) from damaged cells, vacuolation (arrows heads) distortion in mucosal epithelium and detachment of lamina propria. G, H, and I: after 5 weeks of GSH + ME administration showing increasing in vacuolation and lymphocytes aggregation. Scale bar: A, D, and G = 50 μ m; B, E, and H = 10 μ m and C, F, and I = 5 μ m.

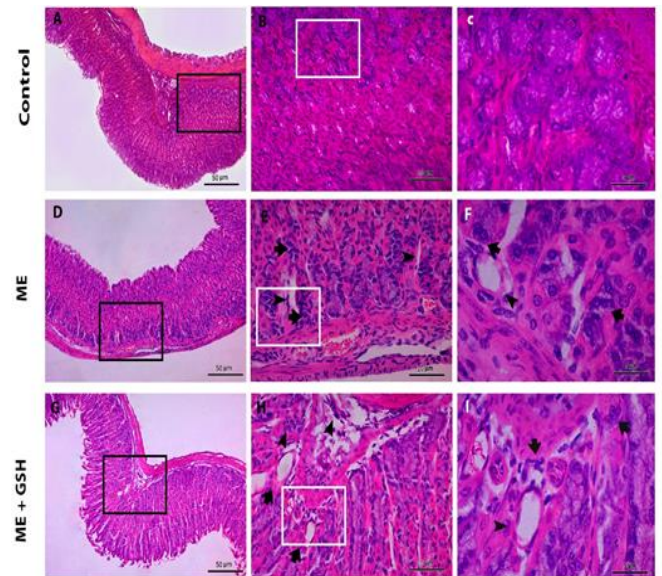


Figure 9: Photomicrographs from sections of pigmented mice stomach stained with H&E. A, B, and C: Control stomach with normal architecture. D, E, and F: After 3 weeks of ME administration showing inflammation with lymphocytes aggregation (arrows) from damaged cells, vacuolation (arrows heads), distortion in mucosal epithelium and detachment of lamina propria. G, H, and I: after 5 weeks of GSH + ME administration showing increasing in vacuolation and lymphocytes aggregation. Scale bar: A, D, and G = 50 μ m; B, E, and H = 10 μ m and C, F, and I = 5 μ m.

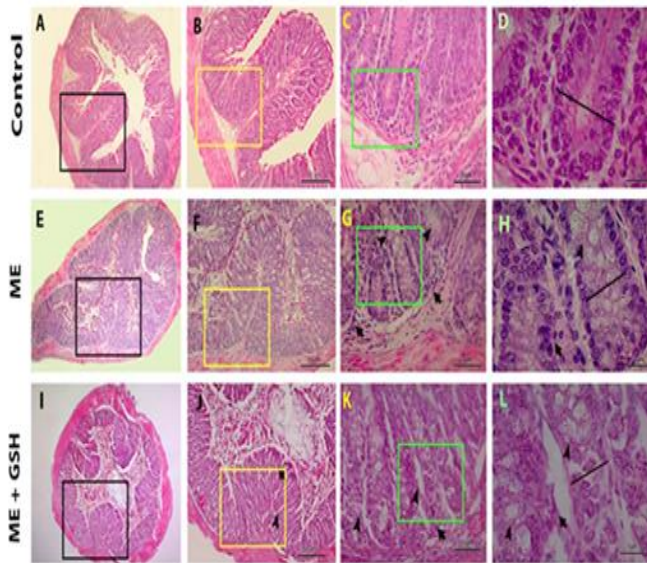


Figure 10: Photomicrographs from sections of albino mice colon stained with H&E. A, B, C, and D: showing control colon with normal architecture. E, F, G, and H: after 3 weeks of ME administration showing inflammation with lymphocytes aggregation (arrows) from damaged cells and vacuolation (arrows heads). I, J, K, and L: after 5 weeks of GSH + ME administration showing increasing in vacuolation and lymphocytes aggregation. Scale bar is 50 mm for A, E, and I 10 mm for B, F, and J, and 5 mm for C, D, G, H, K, and L. Scale bar: A, E, and I = 100 μ m; B, F, and J = 50 μ m and C, G, and K = 10 μ m, and D, H, and L = 5 μ m.

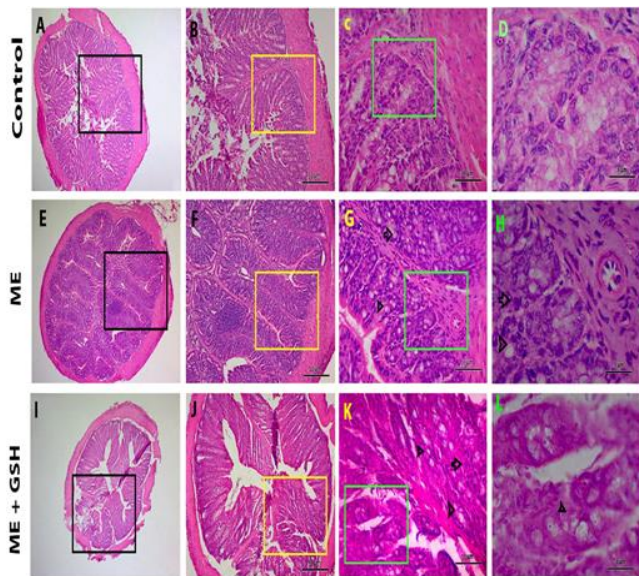


Figure 11: Photomicrographs from sections of pigmented mice colon stained with H&E. A, B, C, and D: showing control colon with normal architecture. E, F, G, and H: after 3 weeks of ME administration-showing inflammation with lymphocytes aggregation (arrows) from damaged cells and vacuolation (arrows heads). I, J, K, and L: after 5 weeks of GSH+ME administration showing increasing in vacuolation and lymphocytes aggregation. Scale bar: A, E, and I = 100 μ m; B, F, and J = 50 μ m and C, G, and K = 10 μ m, and D, H, and L = 5 μ m.

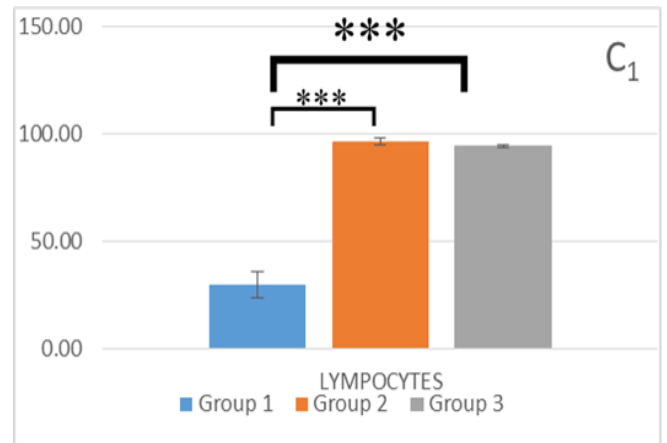
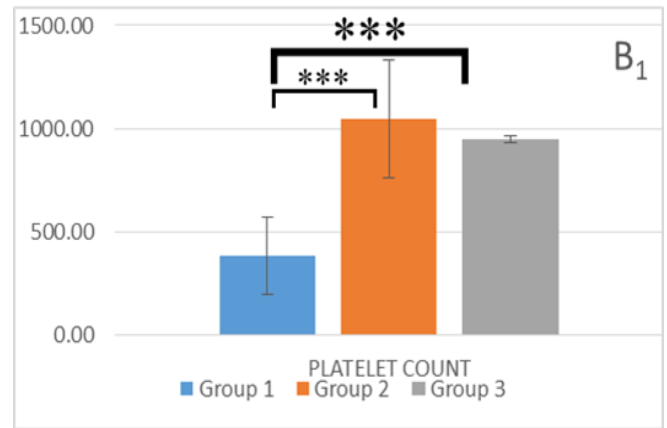
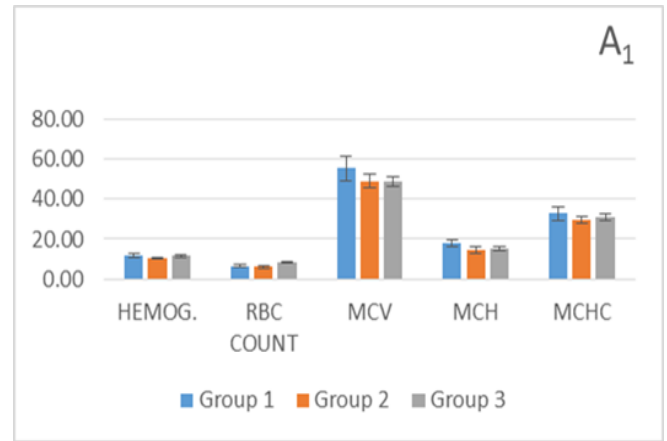


Figure 12: Hematological parameter alternations of albino mice. After three weeks, the ME showing a decrease in HGB, RBC count, MCV, MCHC, and MVC, as well as a significant increase ($p \leq 0.001$) in platelets, and a significant increase ($p \leq 0.001$) in lymphocytes. After 5 weeks of GSH and ME administration, exhibited a rise in HGB, RBC S count, MCV, MCHC, and MVC. However, very significant decreases in platelets ($p \leq 0.001$) as compared to group one and a significant drop in lymphocytes ($p \leq 0.001$) were appeared.

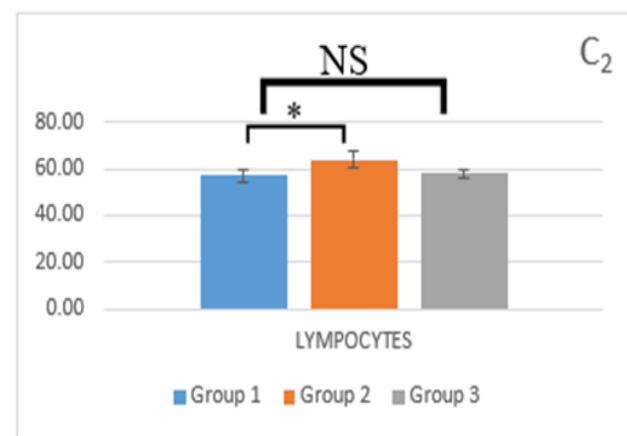
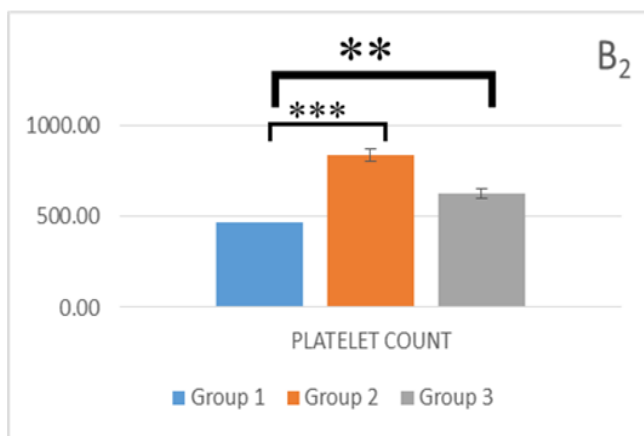
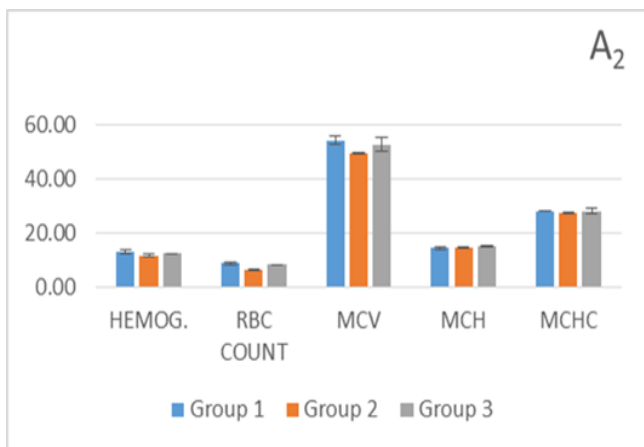


Figure 13: Hematological parameter alternations of pigmented mice. After three weeks, the ME revealed a decrease in HGB, RBC count, MCV, MCHC, and MVC, as well as a substantial rise ($p < 0.001$) in platelets and lymphocytes. After 5 weeks of GSH and ME administration, exhibited a rise in HGB, RBC S count, MCV, MCHC, and MVC. But showing a very significant decrease in platelets ($p \leq 0.01$) as compared to group one, while showing no significant result in lymphocytes.

Regarding to other marine defensive secretion, the ink of sea hares *Aplysia oculifera* and *A. fasciata* induced similar abnormalities caused by ME extract when injected intraperitoneally in mice at levels of 67.8 and 56.4 mg protein/kg [34]. However, a dose (50mg protein/ml) of *Aplysia dactylomela*'s ink displayed degeneration in the hepatocytes, cytoplasmic vacuolation, chromatinolysis, and hypertrophy [35].

Additionally, the extracted toxin azaspiracid from *Patinopecten yessoensis* mussels produced high degeneration and cellular necrosis in the hepatocytes after 24 hours at a dosage of 0.3 mg/kg [36]. On contrast, ME extracted from the fungus *Auricularia auricula* showed a reduction in alcohol-induced liver damage [37]. Furthermore, marine algal toxins (azaspiracid and okadaic acid) in the range from 0.3 to 0.45 mg/kg, caused moderate liver damage and fatty changes in hepatocytes [38]. 25 mg/kg injection of the cone snail *Conus lentiginosus*'s venom produced degeneration of hepatocytes, hemolyzed blood in central veins and developed granulomatous lesions in the perivascular area of treated mice. Constriction of the sinusoidal space and hyperplasia of cortical cells and distinct hepatocyte pyknosis as well as vacuolated regions like honeycombs have been noticed in albino mice treated with venoms of *Conus inscriptus* and *C. lentiginosus* [39].

Regarding the histopathological changes induced in the spleen in this study, ME had induced some histopathological abnormalities such as lymphocytic aggregations and red pulp infiltration, increasing the number of megakaryocytes and distorting the follicle's structure. The growing number of megakaryocytes was in line with the present hematological study that detects noticeably higher platelet counts after ME administrations to both albino and pigmented mice. Megakaryocytes are the cells that produce platelets [40]. Oral administration of the acid secretion of the sea slug *Berthellina citrina* caused atrophy in the white pulp, decrease in the splenocytes density, megakaryocytes cytoplasmic degeneration as well as inflammatory cells infiltrations [41].

In the same context, ink of *A. dactylomela* showed apoptotic splenic macrophages in male mice when injected intraperitoneally with 50 mg protein/ml [42]. Similarly, administration of the marine algal toxin azaspiracids isolated from mussels caused damage to lymphocytes and necrosis in the spleen of mice [36].

The most noticeable hematological indicators in the current study related to a considerable rise in platelets, lymphocytes, and a significant decrease in HGB, RBC count, MCV, MCHC, and MVC. The hemolytic process may have contributed to the significant increase of platelets in this case. As a result, these changes indicated the immunity inhibition as a result of administration of the ME in both types of mice. It is commonly recognized that white blood cells (WBCs) are essential for immunological response and for defending the body against illnesses and external invaders [43 - 45].

Treatment with ME caused inflammation with lymphocyte aggregation from damaged cells, vacuolation deformation in the mucosal epithelium, and lamina propria separation. It also increased vacuolation and lymphocyte aggregation after 5 weeks of GSH and ME treatment. In the intestine, glutathione peroxidases are essential for the detoxification of reactive oxygen species (ROS) generated during inflammation and for the prevention of bacterial colonization [46].

The colon suffered from inflammation, lymphocyte aggregation, lamina propria degeneration and detachment of epithelium after administration with ME. Following GSH and ME treatment, there was a decrease in vacuolation and lymphocyte aggregation compared with normal colon of three weeks after administration. In accordance the extract of marine algae *Gonyaulax monilata* administered orally produced extensive and severe congestion of the abdominal visceral organs [47]. GSH is a water-soluble, low-molecular-weight thiol-tripeptide comprised of three amino acids; glutamate, cysteine, and glycine [48, 49] acts as an antioxidant in the human body is critical in the detoxification of pharmaceuticals, hydrogen peroxide and xenobiotics [21, 22].

Herein, *S. pharaonis* ME caused negative impacts for the mammalian digestive system at the current level (25 mg/kg). Such results are in accordance to the oral administration of a combination of the shellfish toxins yessotoxin and homoyessotoxin which caused degenerative lesions in mice's small intestines [50]. In a mouse model of inflammation-associated carcinogenesis, glutathione peroxidase-2 and selenium reduced inflammation and tumors [51]. Through the inhibition of H₂O₂-mediated activation of the NF-KB and P38 MAPK signaling pathways, which control intestinal inflammation and death, GSH appears to reduce oxidative damage in intestinal epithelial cells [52].

In this work, the histological sections in both albino and pigmented mice demonstrated inflammation and vacuolation after treatments with ME. Tissues showed a reduction in inflammations and abnormal response following GSH and ME injection demonstrating mild vacuolation and lymphocyte aggregation. Furthermore, whether compared to normal skin or after 5 weeks of GSH and ME administration, the hair follicles increased after 3 weeks of administration of ME-only extract. Follicle melanocytes have the ability to function as regulators of hair development in addition to pigmentary cells. So, increasing of melanin and melanocytes causes an increase in the number of hair follicles [53 - 55].

5. Conclusion

The present study revealed that, histopathological abnormalities produced by the oral injection of the ME extracted from *S. pharaonis*' ink in both white and pigmented mice. Some hematological parameters were measured to support these impacts in some organs of mice. After 3 weeks of ME treatment, it was clearly that ME may be somewhat harmful to the mammalian digestive system at

the current dose (25 mg/kg), resulting in inflammation with lymphoid cell aggregation from cell damage and vacuolation deformation at the stomach and colon. Histopathological deteriorations appeared in liver and spleen tissues, but skin showed a rise in hair follicle numbers and some inflammation. Furthermore, GSH reduced inflammation and vacuolation.

The current research introduces new information about the abnormalities produced by ME extracted from *S. pharaonis*' ink and the ameliorative role of GSH as a medication to control melanin biodistribution. Furthermore, our findings pave the path for further research into the utilization of these extracts as prospective medicine.

CRedit authorship contribution statement:

The authors confirm their contribution to the paper as follows: study conception and design: Alaa Moustafa & Aziz Awaad; data collection: Alaa Moustafa, Aziz Awaad and Basma Abd El-Naser; results analysis and interpretation: Alaa Moustafa, Aziz Awaad & Basma Abd El-Naser; draft manuscript preparation: Alaa Moustafa, Aziz Awaad & Basma Abd El-Naser; All authors reviewed the results and approved the final version of the manuscript.

Data availability statement

The data used to support the findings of this study are available from the corresponding author upon request.

Declaration of competing interest

The authors declare that they have no known competing financial interests or personal relationships that could have appeared to influence the work reported in this paper.

References

- [1] M. Hazan, Knopf Inc.; New York, NY, USA: (1992).
- [2] J. A. Marquinet, J. Inaki, *U.S. Patent* (2001) B16,329,010.
- [3] A. Mochizuki, *Bulletin of the Japanese Society of Scientific Fisheries*, 45(1979).
- [4] M. Takai, K. Yamazaki, Y. Kawai, N. Inoue, H. *Bulletin of the Japanese Society of Scientific Fisheries (Japan)*, 59 (1993) 1609-1615.
- [5] N.M. Abraham, H. Spors, A. Carleton, T.W. Margrie, T. Kuner, A.T. Schaefer, *Neuron*, 44 (2004) 865-876.
- [6] N.K. Vate, S.J. Benjakul, *Food Hydrocolloids*, 56 (2016) 62-70.
- [7] B.D. Ulery, L.S. Nair, C.T. Laurencin, *Journal of Polymer Science Part B: Polymer Physics*, 49 (2011) 832-864.
- [8] C.D. Derby, *Marine Drugs*, 12 (2014) 2700-2730.
- [9] J. Chen, Y. Zhou, S. Mueller-Steiner, F. Chen, H. Kwon, S. Yi, L. Mucke, L.J. Gan, *Journal of Biological Chemistry*, 280 (2005) 40364-40374.
- [10] S. Elangovan, S.J. Arumugam, *Aquaculture International*, 31 (2023) 3095-3108.
- [11] Y. Fitriah, I.J. Khusnul Khotimah, *Egyptian Journal of Aquatic Biology and Fisheries*, 25 (2021) 689-704.
- [12] R. Schmidt, M. Knap, D.A. Ivanov, J.S. You, M. Cetina, E.J. Demler, *Reports on Progress in Physics*, 81 (2018) 024401.
- [13] J. Xie, Z. Tong, X. Guan, B. Du, H. Qiu, A.S. Slutsky, *Intensive Care Medicine*, 46 (2020) 837-840.

- [14] S. Ghattavi, A. Homaei, E. Kamrani, D. Saberi, M.J. Daliri, *Progress in Organic Coatings*, 174 (2023) 107327.
- [15] J.L. Ebenezer, R. Shanmugam, A.J. Jayasree, *Journal of Pharmaceutical Negative Results*, 13 (2022) 9280-9286.
- [16] H. Wang, N. Bi, Y. Saito, Y. Wang, X. Sun, J. Zhang, Z.J. Yang, *Journal of Hydrology*, 391 (2010) 302-313.
- [17] M. Sumi, B. Thazeem, K.J. Sunish, *The Journal of Basic and Applied Zoology*, 84 (2023) 5.
- [18] T. Mimura, K. Maeda, T. Terada, Y. Oda, K. Morishita, S.J. Aonuma, P. Bulletin, *Chemical and Pharmaceutical Bulletin*, 33 (1985) 2052-2060.
- [19] H. Dong, W. Song, C. Wang, C. Mu, *BMC Microbiology*, 17 (2017) 1-10.
- [20] R.L. Schroeder, K.L. Double, J.P. Gerber, *Journal of Chemical Neuroanatomy*, 64 (2015) 20-32.
- [21] S. Sonthalia, D. Daulatabad, R.J. Sarkar, *Indian Journal of Dermatology, Venereology, and Leprology*, 82 (2016) 262.
- [22] L. Chasseaud, *Advances in Cancer Research*, 29 (1979) 175-274.
- [23] N. Gorla, E. De Ferreyra, M. Villarruel, O. De Fenos, J. Castro, *British Journal of Experimental Pathology*, 64 (1983) 388.
- [24] Y. Sugimura, K.J. Yamamoto, *Journal of Nutritional Science and Vitaminology*, 44 (1998) 613-624.
- [25] J.K. Kern, D. Geier, J.B. Adams, C. Garver, T. Audhya, M. Geier, *Medical Science Monitor*, 17 (2011) 677-682.
- [26] C.G. Awuchi, E.N. Ondari, C.U. Ogbonna, A.K. Upadhyay, K. Baran, C.O. Okpala, M. Korzeniowska, R.P. Guiné, *Foods*, 10 (2021) 1279.
- [27] S.R. Fahmy, A.M. Soliman, *African Journal of Pharmacy and Pharmacology*, 7 (2013) 1512-1522.
- [28] R. Riad, *Egyptian Journal of Aquatic Biology & Fisheries* 24 (2020) 555 – 590.
- [29] S. Kuroshima, K. Nakajima, M. Sasaki, T. I, Y. Sumita, T. Asahara, I. Asahina, T.J. Sawase, *Stem Cell Research & Therapy*, 10 (2019) 1-13.
- [30] F. Beermann, S. Ruppert, E. Hummler, F. Bosch, G. Müller, U. Rüther, G.J. Schütz, *The EMBO Journal*, 9 (1990) 2819-2826.
- [31] V.J. Hearing, K.J. Tsukamoto, *The FASEB Journal*, 5 (1991) 2902-2909.
- [32] B.S. Larsson, *Pigment Cell Research*, 6 (1993) 127-133.
- [33] K. Urabe, P. Aroca, K. Tsukamoto, D. Mascagna, A. Palumbo, G. Protta, V.J. Heari, *Molecular Cell Research*, 1221 (1994) 272-278.
- [34] A. Y. Moustafa, PhD Thesis, Faculty of Science Sohag, South Valley University (2005).
- [35] Moustafa, A. Y. and Abu-Dief, *Journal of The Egyptian Society for Biotechnology & Environmental Science*, 10 (2007) 235-263.
- [36] E. Ito, M. Satake, K. Ofuji, N. Kurita, T. McMahon, K. James, T.J. Yasumoto, *Toxicon*, 38 (2000) 917-930.
- [37] R. Hou, X. Liu, J. Yan, K. Xiang, X. Lin, G. Chen, M. Zheng, *Food & function*, 10 (2019) 1017-1027.
- [38] E. Ito, M. Satake, K. Ofuji, M. Higashi, K. Harigaya, T. McMahon, T.J. Yasumoto, *Toxicon*, 40 (2002) 193-203.
- [39] P. Kumar, K. Venkateshvaran, P. Srivastava, S. Nayak, S. Shivaprakash, *International Journal of Advanced Research in Pharmaceutical & Bio sciences*, 3 (2013) 1-11.
- [40] A. González-Villalva, G. Piñón-Zárate, A. De la Peña Díaz, M. Flores-García, P. Bizarro-Nevarés, E.P. Rendón- Huerta, L. Colín-Barenque, T.I. Fortoul, *Environmental Toxicology and Pharmacology*, 32 (2011) 447-456.
- [41] A.Awaad, S. El-Saraf and Alaa Moustafa . *Sohag Journal of Science* 9(3), (2024) 308-324.
- [42] A. Y. Moustafa, and Mohamed D. S., *J. Egypt. Ger. Soc. Zool.* (64D), (2012) 1-16.
- [43] H. Liu, Y. Zhang, M. Li, P.J. Luo, *International Journal of Biological Macromolecules*, 140 (2019) 1098-1105.
- [44] A. Davis, D. Maney, J.J. Maerz, *Functional Ecology*, 22 (2008) 760-772.
- [45] D.J. AK, *Functional ecology*, 22 (2008) 760-772.
- [46] F. Chu, R.S. Esworthy, J.H. Doroshov, *Free Radical Biology and Medicine*, 36 (2004) 1481-1495.
- [47] E. Erker, L.J. Slaughter, E.L. Bass, J. Pinion, J. Wutoh, *Toxicon*, 23 (1985) 761-767.
- [48] D.A. Dickinson, H. Forman, *Annals of the New York Academy of Sciences*, 973 (2002) 488-504.
- [49] D.A. Dickinson, H. Forman, *Biochemical pharmacology*, 64 (2002) 1019-1026.
- [50] A. Tubaro, S. Sosa, M. Carbonatto, G. Altinier, F. Vita, M. Melato, M. Satake, T.J. Yasumoto, *Toxicon*, 41 (2003) 783-792.
- [51] S. Krehl, M. Loewinger, S. Florian, A.P. Kipp, A. Banning, L.A. Wessjohann, M.N. Brauer, R. Iori, R.S. Esworthy, F. Chu, *Carcinogenesis*, 33 (2012) 620-628.
- [52] H. Ren, Q. Meng, N. Yepuri, X. Du, J.O. Sarpong, R.N. *Journal of Surgical Research*, 222 (2018) 39-47.
- [53] A. Slominski, R.J. Paus, *Journal of Investigative Dermatology*, 101 (1993) 90-97.
- [54] S.A. D'Mello, G.J. Finlay, B.C. Baguley, M.E. Askarian, *International Journal of Molecular Sciences*, 17 (2016) 1144.
- [55] A. Slominski, J. Wortsman, P.M. Plonka, K.U. Schallreuter, R. Paus, D.J. Tobin, *Journal of Investigative Dermatology*, 124 (2005) 13-21.